*J. Fluid Mech.* (2002), *vol.* 461, *pp.* 301–319.  
DOI: 10.1017/S0022112002008431 Printed in the United Kingdom

# The effect of compressibility on the critical swirl of vortex flows in a pipe

By Z. RUSAK AND J. H. LEE

Department of Mechanical, Aerospace, and Nuclear Engineering, Rensselaer Polytechnic Institute, Troy, NY 12180-3590, USA

(Received 15 June 2001 and in revised form 7 January 2002)

The effect of compressibility on the critical swirl level for breakdown of subsonic vortex flows in a straight circular pipe of finite length is studied. This work extends the critical-state concept of Benjamin (1962) to include the influence of Mach number on the flow behaviour. The analysis is based on a linearized version of the equations for the motion of a steady, axisymmetric, inviscid and compressible swirling flow of a perfect gas. The relationship between the velocity, density, temperature and pressure perturbations to a base columnar flow state are derived. An eigenvalue problem is formulated to determine the first critical level of swirl at which a special mode of a non-columnar small disturbance may appear on the base flow. It is found that when the characteristic Mach number of the base flow tends to zero the eigenvalue problem and the critical swirl are the same as defined by Wang & Rusak (1996*a*, 1997*a*) in their study of incompressible swirling flows in pipes. As the characteristic Mach number is increased, the critical swirl level increases and the flow perturbation expands in the radial direction. As the Mach number is increased toward a certain limit value related to the core size of the vortex, the critical swirl reaches very large values and becomes singular. The present results indicate that the axisymmetric breakdown of high-Reynolds-number compressible vortex flows may be delayed with the increase of the flow Mach number.

## 1. Introduction

High-performance flight vehicles, especially fighter aircraft designed for transonic and supersonic flight, often require combinations of slender bodies and thin, swept-back lifting surfaces with sharp leading and trailing edges. These configurations generate considerable aerodynamic lift forces at subsonic speeds and at high angles of attack, largely due to the induced flow generated by the vortices that are shed from the lifting surfaces and the nose of the configuration. Increasingly, the desire to improve the performance of such vehicles in high-g manoeuvres has lead to the widening of their operational envelope of flight to even higher angles of attack. However, at a certain angle of attack, the cores of the concentrated vortices may suddenly burst near the wing trailing edge. This phenomenon is called vortex breakdown or burst (see Peckham & Atkinson 1957 and Lambourne & Bryer 1962). Further increase of incidence results in the displacement of the breakdown zone along the vortex axis toward the wing apex. When the breakdown point occurs above or in front of the wing mid-chord, it significantly affects the induced flow field around the wing, causes the loss of the lift force, and leads to its stall. This significantly limits the manoeuvres of the aircraft at subsonic Mach numbers of flight. The breakdown phenomenon

may also be unsteady or asymmetric and, therefore, can result in the appearance of undesired asymmetric loading, lateral forces and moments, and can significantly affect the stability of high-g manoeuvres (Delery 1994). Therefore, understanding and predicting the effect of compressibility or Mach number of flight on the breakdown of high-Reynolds-number vortex flows is essential for the operation of modern fighters and the design of future vehicles.

Theoretical analyses of vortex breakdown have concentrated on an incompressible axisymmetric swirling flow in a tube or in a free domain. Several explanations were proposed: the critical-state concept (Benjamin 1962), the solitary trapped-wave approach (Leibovich & Kribus 1990), the special state of a semi-infinite stagnation zone (Keller, Egli & Exley 1985), the analogy to boundary layer separation (Hall 1972), the nature of swirling flow states in a diverging stream tube (Buntine & Saffman 1995), the appearance of hydrodynamic instabilities (Lessen, Singh & Paillet 1974; Lessen & Paillet 1974; Leibovich & Stewartson 1983), and the positive feedback mechanism between the generation of negative azimuthal vorticity and the divergence of stream-function surfaces (Brown & Lopez 1990). Some of the approaches show a possible relationship between the axisymmetric breakdown and the critical-state concept. Other approaches emphasized the importance of an adverse pressure gradient or viscosity in the appearance of a separation (breakdown) zone along the vortex axis.

In a recent set of papers, Wang & Rusak (1996*a*, *b*, 1997*a*, *b*), Rusak, Judd & Wang (1997), Rusak, Wang & Whiting (1998*a*), Rusak, Whiting & Wang (1998*b*) and Rusak (1998, 2000) have presented a theoretical approach which describes the axisymmetric vortex breakdown process. The combination of results from various papers shows that vortex breakdown appears as a result of a nonlinear competition of effects and parameters. The main parameter is the swirl ratio characterizing the vortex flow (Wang & Rusak 1997*a* and Rusak *et al.* 1998*a*, *b*). Other effects include the inviscid instability mechanism of vortex flows (Wang & Rusak 1996*a*, *b*), the viscosity (Wang & Rusak 1997*b*), the adverse pressure gradient (Rusak *et al.* 1997), and the upstream vorticity perturbations (Rusak 1998). The breakdown of high-Reynolds-number vortex flows is a transition from a concentrated vortex flow that becomes unstable when the swirl ratio is above a certain limit level to a flow with a separation (breakdown) zone at a lower level of energy.

Although much progress has been made in the research on the mechanisms of vortex breakdown, none of the previous theoretical studies investigated the effects of flow compressibility or Mach number on the nature of the breakdown of vortex flows. These effects are specifically important in studying the aerodynamic and flow characteristics around wings and airplanes operating at subsonic speeds, where the flight Mach number is not small and may reach values of 0.2 to 0.7. In such cases, compressibility effects may create changes in the thermodynamic properties of the flow and as a result of the balance of mass, momentum and energy may change the nature of the interaction between the velocity components. Such global changes in the flow may modify the critical swirl level for the appearance of vortex breakdown from its incompressible (low Mach number) level to different values, especially when the Mach number is sufficiently high.

Only a limited number of numerical studies has focused on investigating the vortex breakdown in compressible vortex flows. The recent numerical studies by Melville (1996) and Herrada, Prez-Saborid & Barrero (2000) have demonstrated that increasing the characteristic Mach number of the flow results in an increase of the vortex swirl ratio at which breakdown appears for the first time as well as a decrease in the

severity of breakdown at a given swirl ratio. However, there is no theoretical model that describes this behaviour.

The present paper investigates the effect of compressibility on the critical swirl level for breakdown of subsonic vortex flows in a circular pipe of finite length. It is a first step toward developing an understanding of the dynamics of compressible flows with swirl and vortex breakdown. This work extends the critical-state concept of Benjamin (1962) and Wang & Rusak (1996*a*, 1997*a*) to include the influence of Mach number on the flow behaviour. The analysis is based on a linearized version of the equations for the motion of a steady, axisymmetric, inviscid and compressible swirling flow of a perfect gas. An eigenvalue problem is formulated to determine the first critical level of swirl at which a special mode of a non-columnar small disturbance may appear on the base flow. As the characteristic Mach number is increased, the critical swirl level increases and the flow perturbation expands in the radial direction. As the Mach number is increased toward a certain limit value related to the core size of the vortex, the critical swirl reaches very large values and becomes singular. The present results indicate that the breakdown of compressible high-Reynolds-number vortex flows may be delayed with the increase of the flow Mach number.

## 2. Mathematical model

A steady, inviscid, non-heat conducting, compressible axisymmetric flow with swirl of a perfect gas is considered in a finite-length, circular, straight pipe of radius $r_t$. The pipe centreline is the $\bar{x}$-axis where $0 \leqslant \bar{x} \leqslant x_0 r_t$ and the radial distance $\bar{r}$ ranges within $0 \leqslant \bar{r} \leqslant r_t$. The flow thermodynamic properties may be described by the perfect gas equation of state

$$\bar{P} = \bar{\rho} R \bar{T}, \tag{1}$$

and the fields of radial, circumferential and axial velocities $\bar{u}, \bar{v}, \bar{w}$ respectively, are related to the fields of the pressure $\bar{P}$, density $\bar{\rho}$ and temperature $\bar{T}$ through the continuity, momentum and energy equations:

$$(\bar{\rho}\bar{u})_{\bar{r}} + \frac{\bar{\rho}\bar{u}}{\bar{r}} + (\bar{\rho}\bar{w})_{\bar{x}} = 0, \tag{2}$$

$$\bar{\rho}\left(\bar{u}\bar{u}_{\bar{r}} + \bar{w}\bar{u}_{\bar{x}} - \frac{\bar{v}^2}{\bar{r}}\right) = -\bar{P}_{\bar{r}}, \tag{3}$$

$$\left(\bar{u}\bar{v}_{\bar{r}} + \bar{w}\bar{v}_{\bar{x}} + \frac{\bar{u}\bar{v}}{\bar{r}}\right) = 0, \tag{4}$$

$$\bar{\rho}(\bar{u}\bar{w}_{\bar{r}} + \bar{w}\bar{w}_{\bar{x}}) = -\bar{P}_{\bar{x}}, \tag{5}$$

$$\bar{\rho} C_p(\bar{u}\bar{T}_{\bar{r}} + \bar{w}\bar{T}_{\bar{x}}) - (\bar{u}\bar{P}_{\bar{r}} + \bar{w}\bar{P}_{\bar{x}}) = 0. \tag{6}$$

Here, $R$ is the specific gas constant and $C_p$ is the gas specific heat at constant pressure and is assumed constant.

We study the flow in a pipe with a specific set of conditions posed on the boundaries to reflect the physical situation. In order to satisfy the axisymmetric condition, along the pipe centreline $\bar{r} = 0$ we set

$$\bar{u}(\bar{x}, 0) = 0, \quad \bar{v}(\bar{x}, 0) = 0, \quad \bar{w}_{\bar{r}}(\bar{x}, 0) = 0, \quad \bar{T}_{\bar{r}}(\bar{x}, 0) = 0, \quad \bar{P}_{\bar{r}}(\bar{x}, 0) = 0 \tag{7}$$

for $0 \leqslant \bar{x} \leqslant x_0 r_t$. Along the pipe wall $\bar{r} = r_t$, the normal velocity vanishes, i.e. there is no radial velocity:

$$\bar{u}(\bar{x}, r_t) = 0 \tag{8}$$

for $0 \leqslant \bar{x} \leqslant x_0 r_t$. We prescribe at the pipe inlet $\bar{x} = 0$ the profiles of the axial speed, circumferential speed, azimuthal vorticity ($\bar{\eta} = \bar{u}_{\bar{x}} - \bar{w}_{\bar{r}}$) and temperature as

$$\bar{w}(0, \bar{r}) = U_0 w_0\left(\frac{\bar{r}}{r_t}\right), \quad \bar{v}(0, \bar{r}) = \omega U_0 v_0\left(\frac{\bar{r}}{r_t}\right),$$

$$\bar{\eta}(0, \bar{r}) = \frac{U_0}{r_t}\bar{\eta}_0\left(\frac{\bar{r}}{r_t}\right), \quad \bar{T}(0, \bar{r}) = \bar{T}_0 T_0\left(\frac{\bar{r}}{r_t}\right) \tag{9}$$

for $0 \leqslant \bar{r} \leqslant r_t$. Here, $U_0$ is the axial speed at the inlet centreline, $\omega$ is the swirl ratio of the incoming flow, and $\bar{T}_0$ is the temperature along the inlet centreline. The inlet flow is characterized by a Mach number $M_0 = U_0/a_0$, where $a_0$ is the isentropic speed of sound at the inlet centreline, $a_0 = \sqrt{\gamma R \bar{T}_0}$ where $\gamma$ is the ratio of specific heats of the perfect gas (in the examples in § 4 we use air as the working fluid for which $\gamma = 1.4$ at temperatures below 300 K, see Thompson 1988 p. 640). Note that $w_{0\bar{r}}(0) = 0$, $v_0(0) = 0$ and $T_{0\bar{r}}(0) = 0$ should be used for symmetry at the inlet centreline. We also consider in the present paper the case where there is zero axial gradient of the radial speed along the pipe inlet and the inlet azimuthal vorticity is fixed, i.e.

$$\bar{\eta}_0 = -\bar{w}_{0\bar{r}} \quad \text{or} \quad \bar{u}_{\bar{x}}(0, \bar{r}) = 0 \quad \text{for} \quad 0 \leqslant \bar{r} \leqslant r_t. \tag{10}$$

This assumption does not limit the present analysis and results. The effect of general azimuthal vorticity profiles at the inlet is described in Rusak (1998) for an incompressible flow and can be included in the present approach in a similar way but is beyond the scope of this paper. Also, at the inlet centreline the pressure is fixed, i.e.

$$\bar{P}(0, 0) = \bar{P}_0. \tag{11}$$

We assume no radial velocity and no axial gradients of the thermodynamic properties along the pipe outlet at $\bar{x} = x_0 r_t$, in accordance with an expected columnar flow state, i.e.

$$\bar{u}(x_0 r_t, \bar{r}) = 0, \quad \bar{T}_{\bar{x}}(x_0 r_t, \bar{r}) = 0, \quad \bar{\rho}_{\bar{x}}(x_0 r_t, \bar{r}) = 0 \tag{12}$$

for $0 \leqslant \bar{r} \leqslant r_t$.

Similar flow boundary conditions were considered in the analysis of Wang & Rusak (1997*a*) for an incompressible (constant temperature) swirling flow in a finite-length pipe. These conditions reflect the physical situation in an experiment on a high-Reynolds-number compressible flow in a pipe. Similar conditions were also used by Beran (1994) in his unsteady compressible flow simulations of vortex breakdown. The boundary conditions (7)–(12) also formulate a basic problem through which the interaction between the flow swirl and compressibility can be studied and results may shed light on the physics of vortex flows.

A basic steady-state solution of the problem formulated by the above equations (1)–(6) and boundary conditions (7)–(12) is a columnar state where for every Mach

number $M_0$ and swirl level $\omega$,

$$\left.\begin{aligned}
&\bar{w}(\bar{x},\bar{r}) = U_0 w_0\left(\frac{\bar{r}}{r_t}\right), \quad \bar{v}(\bar{x},\bar{r}) = \omega U_0 v_0\left(\frac{\bar{r}}{r_t}\right), \quad \bar{u}(\bar{x},\bar{r}) = 0, \quad \bar{T}(\bar{x},\bar{r}) = \bar{T}_0 T_0\left(\frac{\bar{r}}{r_t}\right), \\
&\bar{P}(\bar{x},\bar{r}) = \bar{P}_0 P_0\left(\frac{\bar{r}}{r_t}\right), \quad P_0\left(\frac{\bar{r}}{r_t}\right) = \exp\left(\gamma M_0^2 \omega^2 \int_0^{(\bar{r}/r_t)} \frac{v_0^2(\bar{r^*}/r_t)}{(\bar{r^*}/r_t) T_0(\bar{r^*}/r_t)}\, \mathrm{d}\left(\frac{\bar{r^*}}{r_t}\right)\right), \\
&\bar{\rho}(\bar{x},\bar{r}) = \bar{\rho}_0 \rho_0\left(\frac{\bar{r}}{r_t}\right), \quad \rho_0\left(\frac{\bar{r}}{r_t}\right) = P_0\left(\frac{\bar{r}}{r_t}\right) \Big/ T_0\left(\frac{\bar{r}}{r_t}\right), \quad \bar{P}_0 = \bar{\rho}_0 R \bar{T}_0
\end{aligned}\right\} \tag{13}$$

for $0 \leqslant \bar{x} \leqslant x_0 r_t$. We use equations (1)–(12) to study the possible appearance of a steady perturbation to the set of columnar states at a fixed subsonic Mach number $0 \leqslant M_0 < 1$. Specifically, we look for the critical level of swirl where such a perturbation appears for the first time as the swirl level is increased.

## 3. Small-disturbance analysis and the critical state

We define $r = \bar{r}/r_t$, $x = \bar{x}/r_t$. A perturbed columnar state may be described by

$$\bar{\rho} = \bar{\rho}_0(\rho_0(r) + \delta_1 \rho_1(x,r) + \cdots), \tag{14}$$

$$\bar{T} = \bar{T}_0(T_0(r) + \delta_1 T_1(x,r) + \cdots), \tag{15}$$

$$\bar{P} = \bar{P}_0(P_0(r) + \delta_1 P_1(x,r) + \cdots), \tag{16}$$

$$\bar{w} = U_0(w_0(r) + \epsilon_1 w_1(x,r) + \cdots), \tag{17}$$

$$\bar{u} = U_0(\epsilon_1 u_1(x,r) + \cdots), \tag{18}$$

$$\bar{v} = U_0(\omega v_0(r) + \epsilon_1 v_1(x,r) + \cdots), \tag{19}$$

where the parameter $0 < \delta_1 \ll 1$ represents perturbations to the thermodynamic properties and the parameter $0 < \epsilon_1 \ll 1$ represents perturbations to the velocity components. Substituting these expressions into (1)–(6) gives the base flow relations and the steady linearized equations of motion of a compressible and inviscid flow:

equation of state

$$O(1)\colon\ P_0 = \rho_0 T_0, \tag{20}$$

$$O(\delta_1)\colon\ P_1 = \rho_1 T_0 + \rho_0 T_1; \tag{21}$$

continuity equation

$$O(\epsilon_1, \delta_1)\colon\ \epsilon_1\left(\rho_{0r} u_1 + \rho_0 u_{1r} + \rho_0 \frac{u_1}{r} + \rho_0 w_{1x}\right) + \delta_1(\rho_{1x} w_0) = 0; \tag{22}$$

$r$-momentum equation

$$O(1)\colon\ P_{0r} = \gamma M_0^2 \rho_0 \omega^2 \frac{v_0^2}{r}, \tag{23}$$

$$O(\gamma M_0^2 \epsilon_1, \gamma M_0^2 \delta_1, \delta_1)\colon\ \gamma M_0^2\left[\epsilon_1\left(\rho_0 w_0 u_{1x} - \frac{2}{r}\omega v_0 \rho_0 v_1\right) - \delta_1\left(\rho_1 \omega^2 \frac{v_0^2}{r}\right)\right] = -\delta_1 P_{1r}; \tag{24}$$

$\theta$-momentum equation

$$O(\epsilon_1):\ \omega u_1 v_{0r} + w_0 v_{1x} + \frac{\omega v_0}{r} u_1 = 0; \tag{25}$$

$x$-momentum equation

$$O(\gamma M_0^2 \epsilon_1, \delta_1):\ \gamma M_0^2 \epsilon_1 (\rho_0 w_{0r} u_1 + \rho_0 w_0 w_{1x}) = -\delta_1 P_{1x}; \tag{26}$$

energy equation

$$O(\epsilon_1, \delta_1):\ \left(\frac{\gamma}{\gamma - 1}\right) [\epsilon_1(\rho_0 u_1 T_{0r}) + \delta_1(\rho_0 w_0 T_{1x})] - [\epsilon_1(u_1 P_{0r}) + \delta_1(w_0 P_{1x})] = 0; \tag{27}$$

where the relation $C_p/R = \gamma/(\gamma - 1)$ has been used.

From the base flow equations (20) and (23), it can be shown that

$$P_0 = \rho_0 T_0, \quad P_{0r} = \gamma M_0^2 \rho_0 \omega^2 \frac{v_0^2}{r}.$$

Then,

$$\frac{P_{0r}}{P_0} = \gamma M_0^2 \omega^2 \frac{v_0^2}{r T_0} \tag{28}$$

and from (9) $P_0(0) = 1$. The solution of (28) gives

$$P_0(r) = \exp\left(\gamma M_0^2 \omega^2 \int_0^r \frac{v_0^2(r^*)}{r^* T_0(r^*)}\, \mathrm{d}r^*\right). \tag{29}$$

The $r$- and $x$-momentum equations (24) and (26) show that

$$\delta_1 = \gamma M_0^2 \epsilon_1. \tag{30}$$

Also, using (9)–(11) and (15)–(19) we find that

$$T_1(0,r) = w_1(0,r) = v_1(0,r) = u_{1x}(0,r) = 0 \quad \text{for} \quad 0 \leqslant r \leqslant 1 \quad \text{and} \quad P_1(0,0) = 0. \tag{31}$$

Applying (21), (24), and (31) at $x = 0$ shows that also

$$P_1(0,r) = \rho_1(0,r) = 0 \quad \text{for} \quad 0 \leqslant r \leqslant 1. \tag{32}$$

Then, using the linearized continuity equation (22), we have

$$\frac{1}{r}(r\rho_0 u_1)_r + (\rho_0 w_1 + \gamma M_0^2 \rho_1 w_0)_x = 0. \tag{33}$$

Let $y = r^2/2$. A perturbation stream function $\psi_1(x, y)$ is defined by

$$\rho_0 u_1 = -\frac{\psi_{1x}}{\sqrt{2y}} \quad \text{and} \quad \rho_0 w_1 = \psi_{1y} - \gamma M_0^2 \rho_1 w_0, \tag{34}$$

where (31) and (32) are used and where $\psi_1(0,r) = 0$ for $0 \leqslant r \leqslant 1$.

Let $K = rv$ be the circulation function and $K_0 = rv_0$ the base-flow circulation function. The linearized $\theta$-momentum equations (25) and (31) show that the perturbation to the circulation function must satisfy

$$K_1 = r v_1 = \frac{\omega K_{0y}}{w_0 \rho_0} \psi_1. \tag{35}$$

Differentiating (24) with respect to $x$ and (26) with respect to $r$, subtracting one

from the other, using relations (30), (34) and (35), and multiplying the result by $(-1/rw_0)$ gives following equation relating $\psi_1$ and $\rho_1$:

$$\psi_{1yyx}+\frac{\psi_{1xxx}}{2y}+\left(\omega^2\frac{K_0K_{0y}}{2y^2w_0^2}-\frac{w_{0yy}}{w_0}\right)\psi_{1x}+\gamma M_0^2\left(\frac{\omega^2K_0^2}{4y^2w_0}\rho_{1x}-2w_{0y}\rho_{1x}-w_0\rho_{1xy}\right)=0. \tag{36}$$

Note that when $M_0=0$ the effect of the density perturbation on the stream function perturbation disappears.

To find another relation between $\rho_{1x}$ and $\psi_1$, we first use (30) and the linearized energy equation (27) which together give

$$\gamma M_0^2\rho_0T_{1x}=\left(\frac{T_{0y}}{w_0}-\frac{\gamma-1}{\gamma}\frac{P_{0y}}{\rho_0w_0}\right)\psi_{1x}+(\gamma-1)M_0^2P_{1x}. \tag{37}$$

Also, from (26) and (34) we have

$$P_{1x}=w_{0y}\psi_{1x}-w_0(\psi_{1xy}-\gamma M_0^2w_0\rho_{1x}). \tag{38}$$

Differentiating (21) with respect to $x$ and using (37) and (38) gives

$$\rho_{1x}=\frac{1}{\gamma M_0^2(T_0-M_0^2w_0^2)}\left[\psi_{1x}\left(M_0^2w_{0y}-\frac{T_{0y}}{w_0}+\frac{\gamma-1}{\gamma}\frac{P_{0y}}{\rho_0w_0}\right)-\psi_{1yx}M_0^2w_0\right]. \tag{39}$$

Also, from (37)–(39) we have

$$P_{1x}=\frac{w_0}{T_0-M_0^2w_0^2}\left[\psi_{1x}\left(\frac{w_{0y}}{w_0}T_0-T_{0y}+\frac{\gamma-1}{\gamma}\frac{P_{0y}}{\rho_0}\right)-\psi_{1xy}T_0\right], \tag{40}$$

$$T_{1x}=\frac{w_0}{\rho_0(T_0-M_0^2w_0^2)}\left[\psi_{1x}\left(\frac{\gamma-1}{\gamma}\frac{w_{0y}}{w_0}T_0+\frac{T_0-\gamma M_0^2w_0^2}{\gamma M_0^2w_0^2}\left(T_{0y}-\frac{\gamma-1}{\gamma}\frac{P_{0y}}{\rho_0}\right)\right)-\psi_{1xy}\frac{\gamma-1}{\gamma}T_0\right]. \tag{41}$$

Substituting (39) into (36), using (28), and defining $\Omega=\omega^2$ gives an equation for the stream function perturbation $\psi_1$:

$$\begin{aligned}&\psi_{1yyx}\frac{T_0}{T_0-M_0^2w_0^2}+\frac{\psi_{1xxx}}{2y}\\&+\psi_{1yx}\left[-\frac{\gamma M_0^2\Omega K_0^2}{4y^2(T_0-M_0^2w_0^2)}+\frac{(T_0-2M_0^2w_0^2)T_{0y}+2M_0^2w_0w_{0y}T_0}{(T_0-M_0^2w_0^2)^2}\right]\\&+\psi_{1x}\left[\Omega\frac{K_0K_{0y}}{2y^2w_0^2}-\frac{w_{0yy}}{w_0}+\frac{\Omega K_0^2}{4y^2w_0}\frac{M_0^2w_{0y}-T_{0y}/w_0+\Omega(\gamma-1)M_0^2K_0^2/(4y^2w_0)}{T_0-M_0^2w_0^2}\right.\\&\left.-\frac{1}{w_0}\left(w_0^2\frac{M_0^2w_{0y}-T_{0y}/w_0+\Omega(\gamma-1)M_0^2K_0^2/(4y^2w_0)}{T_0-M_0^2w_0^2}\right)_y\right]=0.\end{aligned} \tag{42}$$

Here we used $P_{0y}/\rho_0=\gamma M_0^2\Omega K_0^2/4y^2$.

Integrating (42) with respect to $x$ gives

$$\psi_{1yy} + \frac{\psi_{1xx}}{2y}\frac{T_0 - M_0^2 w_0^2}{T_0} + \psi_{1y}\left[-\frac{\gamma M_0^2 \Omega K_0^2}{4y^2 T_0} + \frac{(T_0 - 2M_0^2 w_0^2)T_{0y} + 2M_0^2 w_0 w_{0y} T_0}{(T_0 - M_0^2 w_0^2)T_0}\right]$$
$$+ \psi_1\left[\left(\Omega\frac{K_0 K_{0y}}{2y^2 w_0^2} - \frac{w_{0yy}}{w_0}\right)\frac{T_0 - M_0^2 w_0^2}{T_0}\right.$$
$$+ \frac{\Omega K_0^2}{4y^2 w_0 T_0}\left(M_0^2 w_{0y} - \frac{T_{0y}}{w_0} + \Omega(\gamma - 1)M_0^2\frac{K_0^2}{4y^2 w_0}\right)$$
$$\left. - \frac{T_0 - M_0^2 w_0^2}{w_0 T_0}\left(w_0^2\frac{M_0^2 w_{0y} - T_{0y}/w_0 + \Omega(\gamma - 1)M_0^2 K_0^2/(4y^2 w_0)}{T_0 - M_0^2 w_0^2}\right)_y\right] = 0. \quad (43)$$

The boundary conditions for solving (43) are found from (7)–(13) and (31), (32):

$$\psi_1(x, 0) = 0, \quad \psi_1(x, 1/2) = 0 \quad \text{for} \quad 0 \leqslant x \leqslant x_0, \quad (44)$$

$$\psi_1(0, y) = 0, \quad \psi_{1x}(x_0, y) = 0 \quad \text{for} \quad 0 \leqslant y \leqslant 1/2. \quad (45)$$

The problem formulated by (43) and (44)–(45) is an eigenvalue problem. The theory of partial differential equations shows that such a problem has a non-trivial solution only for a specific set of positive eigenvalues $\Omega = \Omega_1, \Omega_2, \ldots$. Following Wang & Rusak (1996*a*, 1997*a*), we define the first eigenvalue $\Omega = \Omega_1 = \omega_1^2$ as 'the critical swirl ratio for a compressible vortex flow in a finite-length pipe'. A standing small-disturbance wave may appear on the columnar state at the critical swirl level. The solution of this eigenvalue problem is

$$\psi_1 = \psi_{1c}(x, y) = \Phi(y)\sin\left(\frac{\pi x}{2x_0}\right), \quad (46)$$

where $\Phi$ is the eigenfunction that corresponds to the critical state at $\Omega_1$ and both are found from the solution of

$$\Phi_{yy} + \Phi_y\left[-\frac{\gamma M_0^2 \Omega_1 K_0^2}{4y^2 T_0} + \frac{(T_0 - 2M_0^2 w_0^2)T_{0y} + 2M_0^2 w_0 w_{0y} T_0}{(T_0 - M_0^2 w_0^2)T_0}\right]$$
$$+ \Phi\left[\left(\Omega_1\frac{K_0 K_{0y}}{2y^2 w_0^2} - \frac{w_{0yy}}{w_0} - \frac{\pi^2}{8yx_0^2}\right)\frac{T_0 - M_0^2 w_0^2}{T_0}\right.$$
$$+ \frac{\Omega_1 K_0^2}{4y^2 w_0^2 T_0}\left(M_0^2 w_0 w_{0y} - T_{0y} + \Omega_1(\gamma - 1)M_0^2\frac{K_0^2}{4y^2}\right)$$
$$\left. - \frac{T_0 - M_0^2 w_0^2}{w_0 T_0}\left(w_0\frac{M_0^2 w_0 w_{0y} - T_{0y} + \Omega_1(\gamma - 1)M_0^2 K_0^2/(4y^2)}{T_0 - M_0^2 w_0^2}\right)_y\right] = 0 \quad (47)$$

with boundary conditions:

$$\Phi(0) = \Phi(1/2) = 0. \quad (48)$$

It can be seen from the above equations that as $M_0$ tends to zero (with $T_0 = 1$) the problem tends uniformly to the eigenvalue problem for computing the critical swirl for an incompressible (constant temperature) columnar vortex flow in a finite-length

pipe that was defined by Wang & Rusak (1996*a*, 1997*a*). Also, as both $M_0$ tends to zero and $x_0$ tends to infinity, it is found that the present problem is reduced to the eigenvalue problem defined by Benjamin (1962).

Using the solution for $\psi_1$, the flow perturbations are given from (31), (32), (34), (35), (39)–(41) and (46) by

$$u_1 = -\left(\frac{\pi}{2x_0}\right)\frac{\Phi(y)}{\sqrt{2y}\rho_0}\cos\left(\frac{\pi x}{2x_0}\right), \tag{49}$$

$$w_1 = \frac{1}{\rho_0(T_0 - M_0^2 w_0^2)}\left[T_0\Phi_y - \left(M_0^2 w_0 w_{0y} - T_{0y} + \frac{\gamma-1}{\gamma}\frac{P_{0y}}{\rho_0}\right)\Phi\right]\sin\left(\frac{\pi x}{2x_0}\right), \tag{50}$$

$$v_1 = \frac{\omega K_{0y}}{\sqrt{2y}w_0\rho_0}\Phi\sin\left(\frac{\pi x}{2x_0}\right), \tag{51}$$

$$\rho_1 = \frac{1}{\gamma M_0^2 w_0(T_0 - M_0^2 w_0^2)}\left[\left(M_0^2 w_0 w_{0y} - T_{0y} + \frac{\gamma-1}{\gamma}\frac{P_{0y}}{\rho_0}\right)\Phi - M_0^2 w_0^2\Phi_y\right]\sin\left(\frac{\pi x}{2x_0}\right), \tag{52}$$

$$P_1 = \frac{w_0}{T_0 - M_0^2 w_0^2}\left[\left(\frac{w_{0y}}{w_0}T_0 - T_{0y} + \frac{\gamma-1}{\gamma}\frac{P_{0y}}{\rho_0}\right)\Phi - T_0\Phi_y\right]\sin\left(\frac{\pi x}{2x_0}\right), \tag{53}$$

$$T_1 = \frac{w_0}{\rho_0(T_0 - M_0^2 w_0^2)}\left[\left(\frac{\gamma-1}{\gamma}\frac{w_{0y}}{w_0}T_0 + \frac{T_0 - \gamma M_0^2 w_0^2}{\gamma M_0^2 w_0^2}\left(T_{0y} - \frac{\gamma-1}{\gamma}\frac{P_{0y}}{\rho_0}\right)\right)\Phi - \frac{\gamma-1}{\gamma}T_0\Phi_y\right]\sin\left(\frac{\pi x}{2x_0}\right). \tag{54}$$

Here $P_{0y}/\rho_0 = \gamma M_0^2\Omega_1 K_0^2/4y^2$.

## 4. Results

We first study the case where the inlet axial velocity and temperature profiles are uniform, $w_0 = T_0 = 1$, and the circumferential velocity is given by a solid-body rotation profile:

$$v_0 = r \quad \text{or} \quad K_0 = 2y. \tag{55}$$

Then, the eigenvalue equation for determining the critical swirl becomes

$$\Phi_{yy} - \Phi_y(\gamma M_0^2\Omega_1) + \Phi\left[\left(\frac{2\Omega_1}{y} - \frac{\pi^2}{8x_0^2 y}\right)(1 - M_0^2) + (\gamma-1)\Omega_1^2 M_0^2\right] = 0 \tag{56}$$

with the boundary conditions (48). This is an ordinary differential equation that can be solved by canned program like Matlab or Maple for $0 \leqslant M_0 < 1$ using a shooting method. In all cases we choose $\Phi_y(0) = 1$ to be the slope at $y = 0$.

Figure 1 shows the computed values of the critical swirl $\omega_1$ as function of Mach number. It can be seen that $\omega_1$ increases with Mach number. As $M_0$ approaches a certain limit value $M_{0\ limit} \sim 0.925$, $\omega_1$ becomes singular. The corresponding critical eigenfunctions $\Phi$ for various Mach numbers are shown in figure 2. It can be seen that as the Mach number is increased the perturbation becomes stronger and expands in the radial direction. This is particularly clear from the functions $\Phi_y$ shown in figure 3.

The axial speed perturbation $-w_1$ and the temperature perturbation $-T_1$ which correspond to the critical state in each case are computed from (50) and (54) and

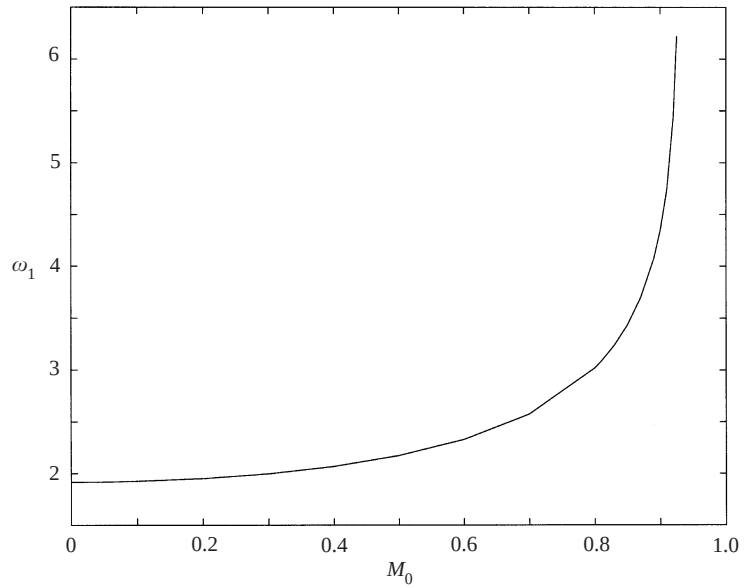


FIGURE 1. The effect of Mach number on the critical swirl number $\omega_1$ of a solid-body rotation ($x_0 = 60.0$).

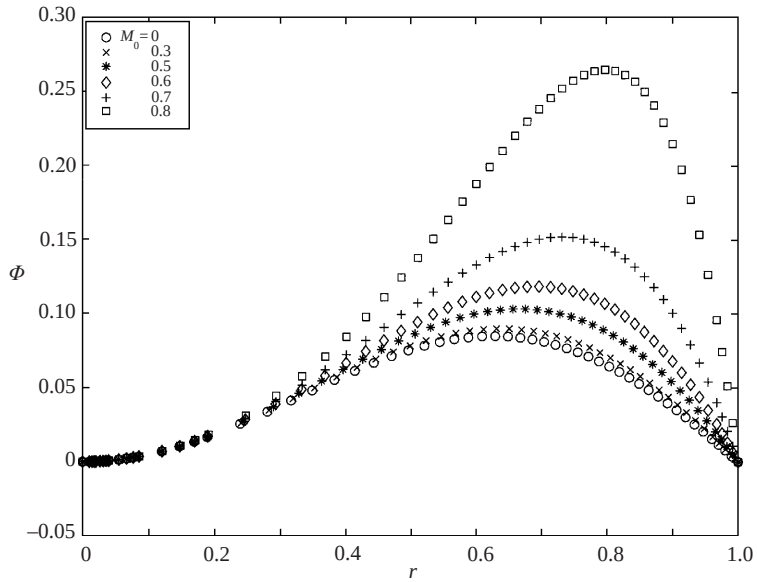


FIGURE 2. The critical eigenfunction $\Phi$ of a solid-body rotation for various Mach numbers ($x_0 = 60.0$).

shown in figures 4 and 5. Note that the negative values of $w_1$ and $T_1$ are used since from the incompressible case it is expected that $\epsilon_1$ in (14)–(19) and (30) is negative. It can be seen that the axial speed deceleration near the centreline and the related temperature increase (which results from the balance of energy) are significantly increased with the increase of Mach number $M_0$. On the other hand, the axial speed acceleration near the wall (resulting from the balance of mass in the pipe) and the

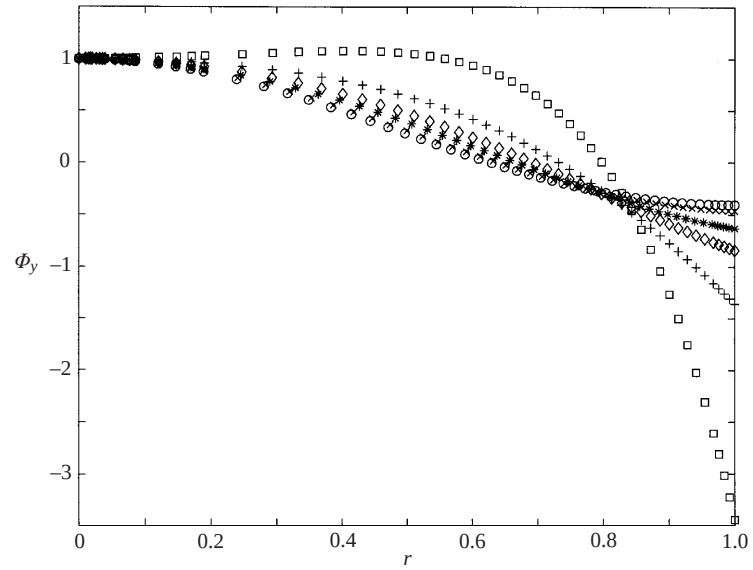


FIGURE 3. The derivative of the critical function $\Phi_y$ of a solid-body rotation for various Mach numbers ($x_0 = 60.0$). Symbols as figure 2.

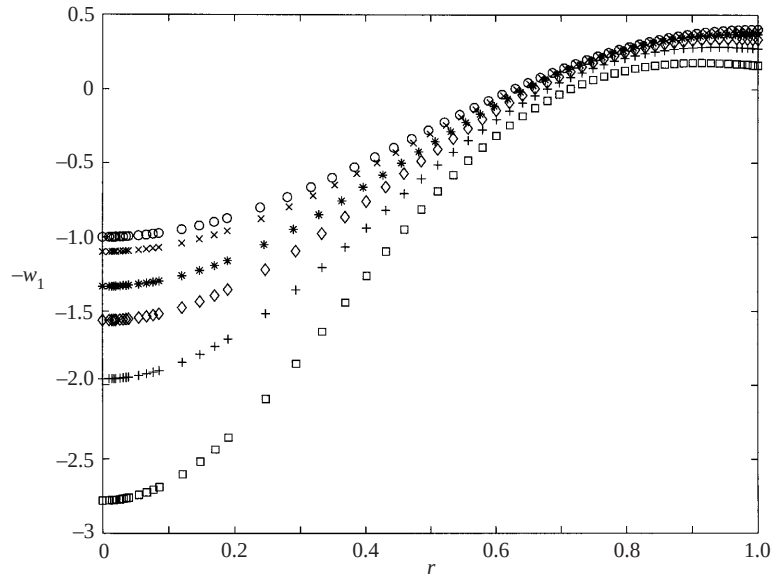


FIGURE 4. The critical axial speed perturbation ($-w_1$) of a solid-body rotation for various Mach numbers ($x_0 = 60.0$). Symbols as figure 2.

related temperature decrease (which results from the balance of energy) are reduced with the increase of Mach number.

In the second case we study a Burgers vortex profile. We again assume that the inlet axial velocity and temperature profiles are uniform, $w_0 = T_0 = 1$, and that the circulation is given by

$$K_0 = 1 - \mathrm{e}^{-2by}. \tag{57}$$

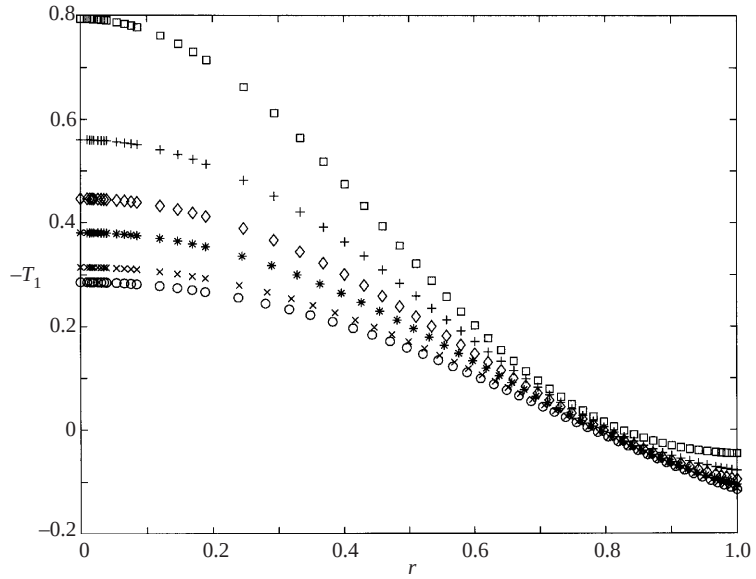


FIGURE 5. The critical temperature perturbation ($-T_1$) of a solid-body rotation for various Mach numbers ($x_0 = 60.0$). Symbols as figure 2.

Here $b$ is a parameter related to the size of the vortex core radius, $r_c/r_t = 1.12/\sqrt{b}$. Then, the eigenvalue equation for determining the critical swirl becomes

$$\Phi_{yy} - \Phi_y \left[\frac{\gamma M_0^2 \Omega_1 (1 - \mathrm{e}^{-2by})^2}{4y^2}\right] + \Phi \left[-\frac{\pi^2}{8yx_0^2}(1 - M_0^2) + (1 - \gamma M_0^2)\frac{b\Omega_1}{y^2}\mathrm{e}^{-2by}(1 - \mathrm{e}^{-2by}) + (\gamma - 1)M_0^2 \frac{\Omega_1}{2y^2}(1 - \mathrm{e}^{-2by})^2 \left(\frac{1}{y} + \frac{\Omega_1}{8y^2}(1 - \mathrm{e}^{-2by})^2\right)\right] = 0 \quad (58)$$

with the boundary conditions from (48)

$$\Phi(0) = \Phi(1/2) = 0. \quad (59)$$

We concentrate on a case where $x_0 = 60.0$. Figure 6 shows the computed values of the critical swirl $\omega_1$ as function of Mach number for various values of $b$ (the core size parameter). It can be seen that as the Mach number $M_0$ is increased from zero to about 0.7 the critical swirl ratio of the flow increases significantly. For example, for the case with $b = 4$, increasing the Mach number from 0 to 0.6 and then to 0.66 results in an increase of the critical swirl ratio from 0.883 to 1.420 and to 1.902, respectively. Also, as the Mach number approaches a certain limit value $M_{0\ limit}$, which weakly depends on $b$, the critical swirl reaches very large values and becomes singular and no solution of the critical swirl can be found for $M_0 > M_{0\ limit}$. For example, when $b = 1.254$ it is found that $M_{0\ limit} \sim 0.695$, when $b = 4$ then $M_{0\ limit} \sim 0.688$, and when $b = 100$ then $M_{0\ limit} \sim 0.684$. Note that $M_{0\ limit}$ slightly decreases as $b$ increases or the vortex core radius $r_c$ decreases.

The corresponding critical eigenfunctions $\Phi(y)$ in the case where $b = 4$ for various Mach numbers are shown in figure 7. It can be seen that as the Mach number is increased the perturbation becomes stronger and expands in the radial direction (see also the related functions $\Phi_y$ for the case $b = 4$ shown in figure 8). The axial

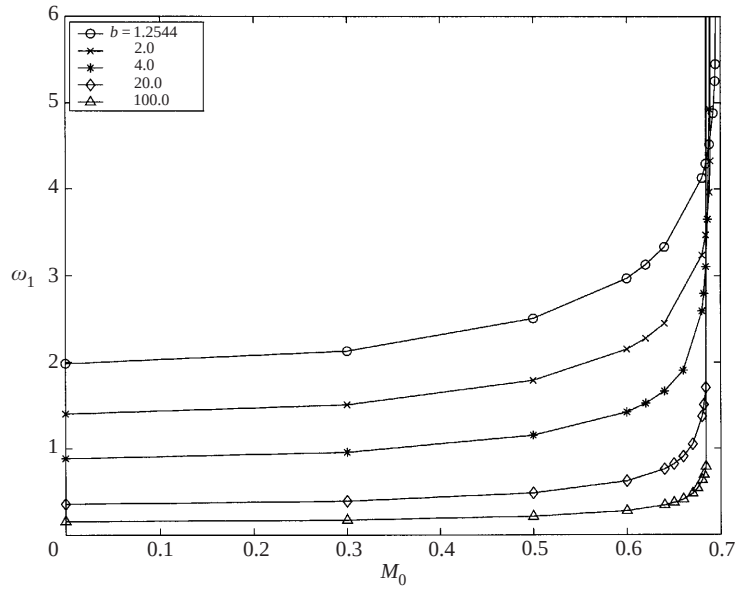


FIGURE 6. The effect of Mach number on the critical swirl number $\omega_1$ of a Burgers vortex with $x_0 = 60.0$.

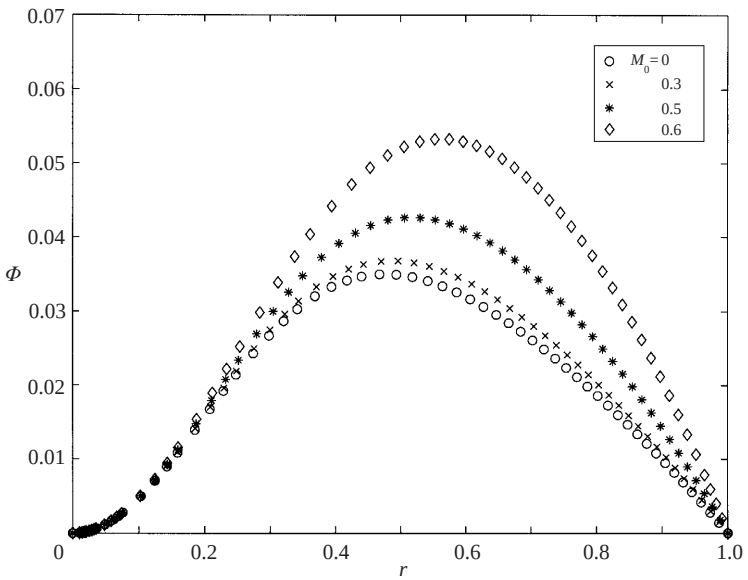


FIGURE 7. The critical eigenfunction $\Phi$ of a Burgers vortex with $b = 4.0$ and $x_0 = 60.0$ for various Mach numbers.

speed perturbation $-w_1$ and the temperature perturbation $-T_1$ which correspond to the critical state in each case are computed from (50) and (54) and shown in figures 9 and 10 for the case $b = 4$. The axial speed deceleration and the related temperature increase near the centreline are significantly increased with the increase of Mach number $M_0$. On the other hand, the axial speed acceleration and the related temperature decrease near the wall are reduced with the increase of Mach number.

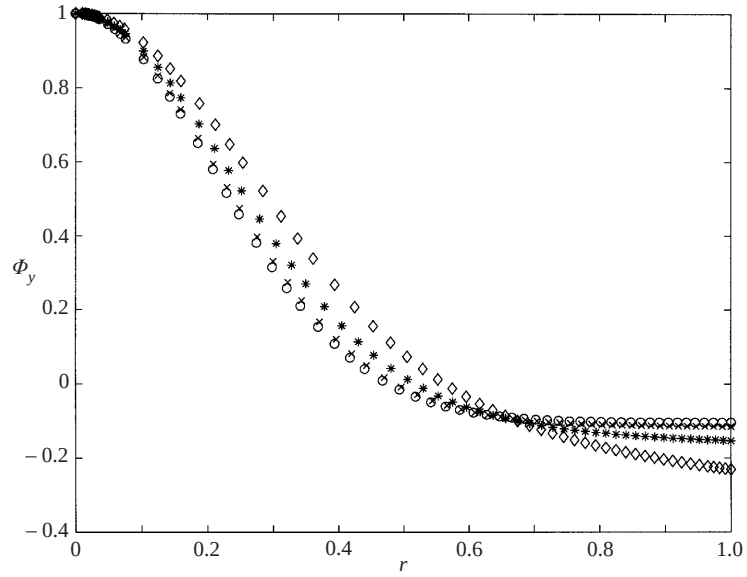


FIGURE 8. The derivative of the critical function $\Phi_y$ of a Burgers vortex with $b = 4.0$ and $x_0 = 60.0$ for various Mach numbers. Symbols as figure 7.

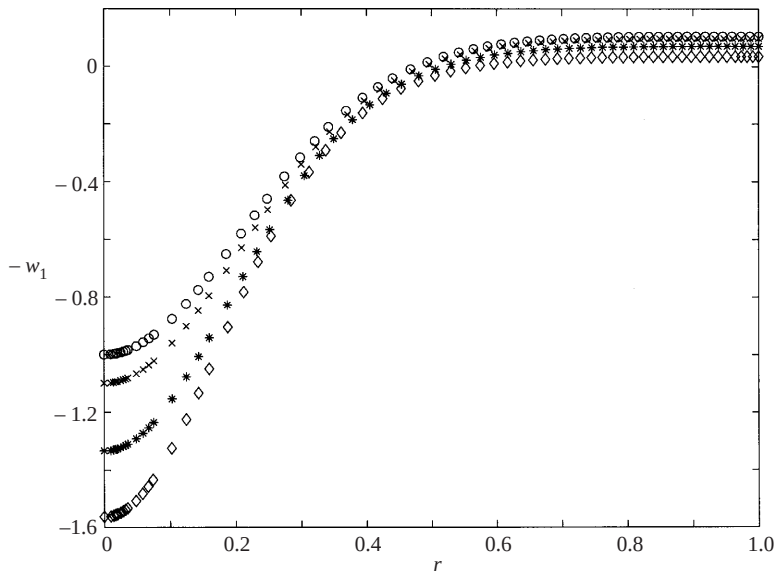


FIGURE 9. The critical axial speed perturbation $(-w_1)$ of a Burgers vortex with $b = 4.0$ and $x_0 = 60.0$ for various Mach numbers. Symbols as figure 7.

The effect of changing the vortex core radius (by changing the parameter $b$) on the critical swirl ratio $V_{max}/w_0 = 0.63817\omega_1\sqrt{b}$ (where $V_{max}$ is the maximum value of $\omega v_0$ found at $r = 1.12/\sqrt{b}$) is demonstrated in figure 11 for various Mach numbers. It can be seen that the critical swirl ratio increase with Mach number for every fixed core radius. Also, for a fixed Mach number the critical swirl increases with the increase of

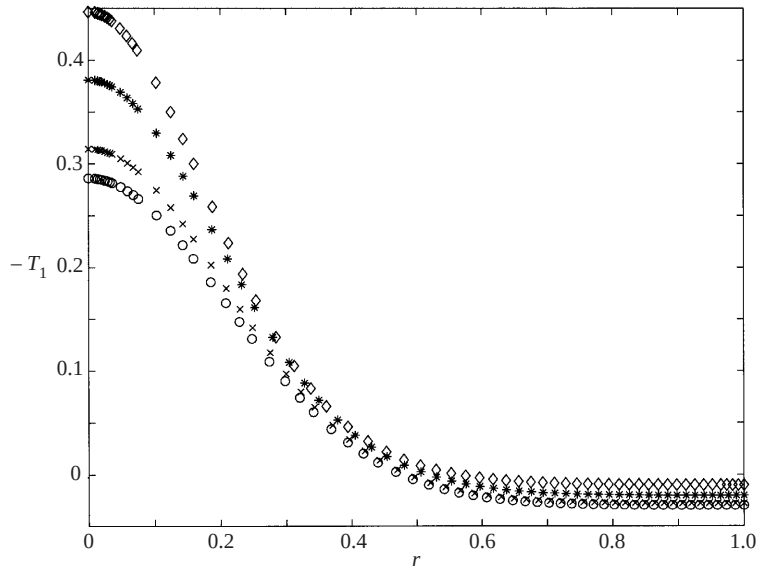


FIGURE 10. The critical temperature perturbation ($-T_1$) of a Burgers vortex with $b = 4.0$ and $x_0 = 60.0$ for various Mach numbers. Symbols as figure 7.

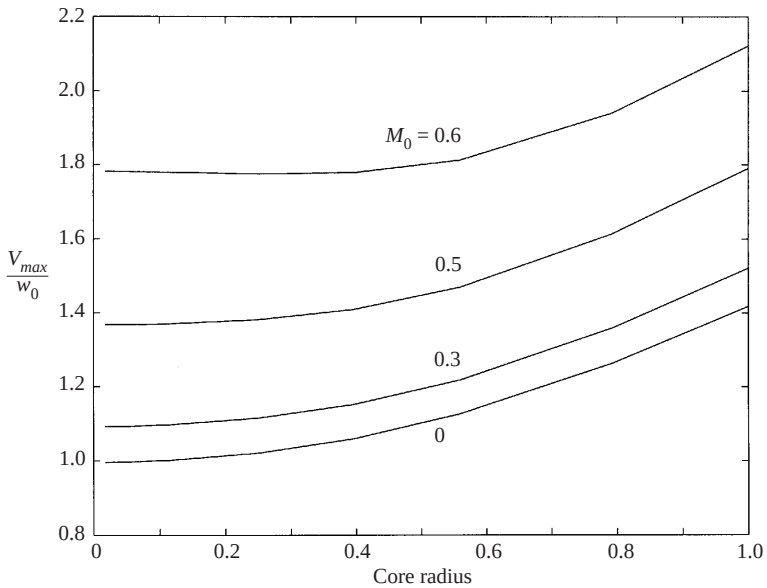


FIGURE 11. The change of $V_{max}/w_0$ with the vortex core radius for various Mach numbers ($x_0 = 60.0$).

the vortex core size. Moreover, note that as the core radius tends to zero the critical level for a fixed Mach number approaches a certain limit value. This limit value of the critical swirl ratio for a vortex with a very thin core may be the critical swirl of a vortex with a finite core size in a pipe with an infinitely large radius, i.e. of a free vortex.

## 5. Conclusions and discussion

The effect of compressibility on the critical swirl level for breakdown of subsonic vortex flows in a circular pipe of finite length can be studied by a small perturbation analysis. This work provides for the first time a theoretical analysis of the effect of the flow Mach number on the critical swirl ratio. It extends the critical-state concept of Benjamin (1962) to include the influence of Mach number on the flow behaviour. It is found that when the characteristic Mach number of the base flow tends to zero the eigenvalue problem and the critical swirl tend uniformly to that defined by Wang & Rusak (1996*a*, 1997*a*) in their study of incompressible swirling flows in pipes. As the characteristic Mach number is increased, the critical swirl level increases and the flow perturbation expands in the radial direction. As the Mach number is increased toward a certain limit value, which is related to the core size of the vortex, the critical swirl reaches very large values and becomes singular. The limit Mach number may be associated with the appearance of transonic effects which are beyond the scope of this paper. For a fixed Mach number, the critical swirl ratio decreases with the decrease in the vortex core radius and approaches a certain limit value as the core size tends to zero. This limit value may be used to estimate the critical swirl of a free vortex of a finite core size at a given characteristic Mach number.

Moreover, the present analysis shows that unlike the physical effects of small viscosity, pipe divergence and inlet vorticity perturbations which were analysed in Wang & Rusak (1997*b*), Rusak *et al.* (1998), and Rusak (1998) and which tend to reduce the critical swirl, the flow compressibility shifts the critical (bifurcation) swirl to higher values and keeps the transcritical nature of bifurcation, as in the case for an incompressible flow. Such a crucial aspect of the dynamical behaviour of such flows was not and cannot be predicted from numerical simulations or any previous study.

The increase of the critical swirl ratio with Mach number may be explained by the following arguments. The vorticity transport equation for a compressible, and inviscid flow is (see Thompson 1988, p. 73)

$$\left(\frac{\bar{\boldsymbol{\omega}}}{\bar{\rho}}\right)_{\bar{t}} + \bar{\boldsymbol{V}} \cdot \nabla \left(\frac{\bar{\boldsymbol{\omega}}}{\bar{\rho}}\right) = \left(\frac{\bar{\boldsymbol{\omega}}}{\bar{\rho}}\right) \cdot \nabla \bar{\boldsymbol{V}} + \frac{1}{\bar{\rho}} \left(\nabla \bar{T} \times \nabla \bar{s}\right), \tag{60}$$

where $\bar{\boldsymbol{V}}$ is the velocity vector and $\bar{\boldsymbol{\omega}} = \nabla \times \bar{\boldsymbol{V}}$ is the vorticity. Here we denote as $\bar{\zeta}$, $\bar{\eta}$, $\bar{\xi}$ the radial, azimuthal and axial components of the vorticity. The specific entropy is $\bar{s}$. This equation describes the balance between the unsteady changes of $\bar{\boldsymbol{\omega}}/\bar{\rho}$, the convection of $\bar{\boldsymbol{\omega}}/\bar{\rho}$, the stretching and tilting of $\bar{\boldsymbol{\omega}}/\bar{\rho}$, and the vorticity production resulting from gradients of the thermodynamic properies of the flow such as the temperature and specific entropy (a baroclinic effect). For an axisymmetric and steady flow in a cylindrical coordinate system this equation for the azimuthal vorticity $\bar{\eta}$ becomes

$$\bar{w}\left(\frac{\bar{\eta}}{\bar{\rho}}\right)_{\bar{x}} + \bar{u}\left(\frac{\bar{\eta}}{\bar{\rho}}\right)_{\bar{r}} + \frac{\bar{v}}{\bar{r}}\left(\frac{\bar{\zeta}}{\bar{\rho}}\right) = \frac{\bar{\zeta}}{\bar{\rho}}\bar{v}_{\bar{r}} + \frac{\bar{\xi}}{\bar{\rho}}\bar{v}_{\bar{x}} + \frac{\bar{\eta}}{\bar{\rho}}\left(\frac{\bar{u}}{\bar{r}}\right) + \frac{1}{\bar{\rho}}\left(\bar{T}_{\bar{x}}\bar{s}_{\bar{r}} - \bar{T}_{\bar{r}}\bar{s}_{\bar{x}}\right). \tag{61}$$

Using the relations for axisymmetric flow $\bar{\zeta} = -\bar{v}_{\bar{x}}$ and $\bar{\xi} = (\bar{r}\bar{v})_{\bar{r}}/\bar{r}$ and letting $\bar{\eta} = \bar{r}\bar{\chi}$ we find that (61) takes the form

$$\bar{w}\left(\frac{\bar{\chi}}{\bar{\rho}}\right)_{\bar{x}} + \bar{u}\left(\frac{\bar{\chi}}{\bar{\rho}}\right)_{\bar{r}} = \frac{1}{\bar{\rho}\bar{r}^4}(\bar{K}^2)_{\bar{x}} + \frac{1}{\bar{\rho}\bar{r}}\left(\bar{T}_{\bar{x}}\bar{s}_{\bar{r}} - \bar{T}_{\bar{r}}\bar{s}_{\bar{x}}\right). \tag{62}$$

Using Gibbs equation $\bar{T}\,\mathrm{d}\bar{s} = C_p\,\mathrm{d}\bar{T} - \mathrm{d}\bar{P}/\bar{\rho}$ and the radial and axial momentum

equations (3) and (5), we find that

$$\left.\begin{aligned} \bar{s}_{\bar{r}} &= C_p \frac{\bar{T}_{\bar{r}}}{\bar{T}} + \frac{1}{\bar{T}}\left(\bar{u}\bar{u}_{\bar{r}} + \bar{w}\bar{u}_{\bar{x}} - \frac{\bar{K}^2}{\bar{r}^3}\right), \\ \bar{s}_{\bar{x}} &= C_p \frac{\bar{T}_{\bar{x}}}{\bar{T}} + \frac{1}{\bar{T}}\left(\bar{u}\bar{w}_{\bar{r}} + \bar{w}\bar{w}_{\bar{x}}\right). \end{aligned}\right\} \tag{63}$$

Also, from the circumferential momentum equation (4) we have $\bar{K}_{\bar{x}} = -\bar{K}_{\bar{r}}\bar{u}/\bar{w}$. Then, (62) becomes

$$\bar{w}\left(\frac{-\bar{\chi}}{\bar{\rho}}\right)_{\bar{x}} + \bar{u}\left(\frac{-\bar{\chi}}{\bar{\rho}}\right)_{\bar{r}} = \frac{2\bar{K}\bar{K}_{\bar{r}}\bar{u}}{\bar{\rho}\bar{w}\bar{r}^4} + \frac{\bar{K}^2}{\bar{\rho}\bar{r}^4}\frac{\bar{T}_{\bar{x}}}{\bar{T}} + \frac{1}{\bar{\rho}\bar{T}\bar{r}}\left(\bar{T}_{\bar{r}}\left(\bar{u}\bar{w}_{\bar{r}} + \bar{w}\bar{w}_{\bar{x}}\right) - \bar{T}_{\bar{x}}\left(\bar{u}\bar{u}_{\bar{r}} + \bar{w}\bar{u}_{\bar{x}}\right)\right). \tag{64}$$

Equation (64) shows that the convection of the property $(-\bar{\chi}/\bar{\rho})$ is balanced by several terms on the right-hand side. The first term represents a stretching effect resulting from the swirl and radial velocities and the density. The second term represents a baroclinic effect resulting from the interaction between the swirl, density and axial temperature gradient. Note that both terms are functions of the square of the swirl level $\omega^2$ and of the inverse of density $1/\bar{\rho}$. The third term also represents a baroclinic effect which results from the radial and axial velocity components, density and radial and axial temperature gradients.

Using the vorticity transport equation (64) and the asymptotic expansions (14)–(19) we can derive (42) and the resulting equation (43) (this is an alternative way to derive these equations). This shows that (42) or (43) are essentially a linearized version of the steady vorticity transport equation (64). The present small-disturbance analysis in § 3 showed that under the given boundary conditions (7)–(12) the steady linearized vorticity transport equation (43) with conditions (44)–(45) has a non-trivial solution only at certain levels of swirl, and specifically at $\omega_1$, the critical swirl for a copmressible vortex flow in a finite-length pipe. A standing small-disturbance wave may appear on the columnar state at the critical swirl. In order to clarify the possible physical meaning of the critical swirl, we refer to the stability study of Wang & Rusak (1996*a*). They showed that the critical swirl for an incompressible and inviscid vortex flow (where $\bar{\rho}$ = constant and no baroclinic effects appear in (64)) is a level of change of stability for the base columnar flow. When $0 \leqslant \omega < \omega_1$, the flow is characterized by a decaying mode of perturbation since the convective effects of the property $(-\bar{\chi})$ dominate the other effects. At the critical swirl ratio $\omega_1$, the vortex state has a neutral mode of perturbation which results from a critical balance between the convective effects and the stretching effects which result from the swirl. When $\omega > \omega_1$, the stretching effects due to swirl dominate the convection of $(-\bar{\chi})$, interact with the inlet conditions, and result in an unstable mode of perturbation which is related to the critical eigenfunction. This unstable mode initiates the axisymmetric vortex breakdown process (see Wang & Rusak 1997*a* and Rusak *et al.* 1998*a* for more details). Although not proven yet, it is strongly expected that a similar behaviour characterizes a compressible vortex flow as the swirl is changed around its critical level, i.e. the critical swirl for a compressible and inviscid flow is also a level of change of stability for the base columnar vortex flow.

Moreover, when (14)–(19) are used and $T_0(r) = 1$ is assumed, it can be shown that the third term on the right-hand side of (64) is on the order of $\epsilon_1^2$, much smaller than the other terms in (64), and may be neglected. Then, the first two terms on the right-hand side of (64) show that the change of density $\bar{\rho}$ in the compressible

case may also affect the level of swirl for a critical balance. In this case, a flow perturbation with a positive radial speed ($\bar{u} > 0$) creates an axial speed deceleration near the pipe centreline and a related increase in the temperature, $\overline{T}_x > 0$, near the centreline. Since in a steady compressible subsonic flow the specific entropy $\bar{s}$ stays constant along a streamline, the density $\bar{\rho}$ also increases near the centreline. These changes increase with the increase of the flow Mach number and affect the size of the stretching and baroclinic effects in the terms in (64). Therefore, a higher level of the swirl ratio $\omega$ is needed to create a critical balance. This means that the critical swirl $\omega_1$ increases with the increase of compressibility effects in the flow and as the characteristic Mach number $M_0$ is increased from a near zero value to finite values. The computed examples in § 4 demonstrate this result.

The theory of Wang & Rusak (1997*a*) also showed that the breakdown of an incompressible vortex flow is strongly related to the critical level of swirl $\omega_1$. Again, although not proven yet for the compressible flow case, there are strong reasons to believe that this behaviour of vortex flows is similar when the flow is compressible. Therefore, the present results indicate that the breakdown of compressible high-Reynolds-number vortex flows may be delayed to higher swirl ratios with the increase of the flow Mach number. This result becomes particularly important when the Mach number is above 0.3 and may be relevant in the design of future high-performance flight vehicles as well as turbo-machinery technologies.

This research was carried out with the support of the National Science Foundation under Grant CTS-9804745.

## REFERENCES

Benjamin, T. B. 1962 Theory of the vortex breakdown phenomenon. *J. Fluid Mech.* **14**, 593–629.

Beran, P. S. 1994 The time-asymptotic behaviour of vortex breakdown in tubes. *Computers Fluids* **23**, 913–937.

Brown, G. L. & Lopez, J. M. 1990 Axisymmetric vortex breakdown. Part 2. Physical mechanisms. *J. Fluid Mech.* **221**, 553–576.

Buntine, J. D. & Saffman, P. G. 1995 Inviscid swirling flows and vortex breakdown. *Proc. R. Soc. Lond.* A **449**, 139–153.

Delery, J. M. 1994 Aspects of vortex breakdown. *Prog. Aerospace Sci.* **30**, 1–59.

Hall, M. G. 1972 Vortex breakdown. *Annu. Rev. Fluid Mech.* **4**, 195–217.

Herrada, M. A., Prez-Saborid, M. & Barrero, A. 2000 Effects of compressibility on vortex breakdown. *Bull. Am. Phys. Soc.* **45** (9), November, p. 122.

Keller, J. J., Egli, W. & Exley, W. 1985 Force- and loss-free transitions between flow states. *Z. Angew. Math. Phys.* **36**, 854–889.

Lambourne, N. C. & Bryer, D. W. 1962 The bursting of leading-edge vortices – some observations and discussion of the phenomenon. *Aero. Res. Counc. R & M* 3282, pp. 1–36.

Leibovich, S. & Kribus, A. 1990 Large amplitude wavetrains and solitary waves in vortices. *J. Fluid Mech.* **216**, 459–504.

Leibovich, S. & Stewartson, K. 1983 A sufficient condition for the instability of columnar vortices. *J. Fluid Mech.* **126**, 335–356.

Lessen, M. & Paillet, F. 1974 The stability of a trailing line vortex. Part 2. Viscous theory. *J. Fluid Mech.* **65**, 769–779.

Lessen, M., Singh, P. J. & Paillet, F. 1974 The stability of a trailing line vortex. Part 1. Inviscid theory. *J. Fluid Mech.* **63**, 753–763.

Melville, R. 1996 The role of compressibility in free vortex breakdown. *AIAA Paper* 96-2075.

Peckham, D. H. & Atkinson, S. A. 1957 Preliminary results of low speed wind tunnel tests on a gothic wing of aspect ratio 1.0. *Aero. Res. Counc.* CP508.

RUSAK, Z. 1998 The interaction of near-critical swirling flows in a pipe with inlet vorticity perturbations. *Phys. Fluids* **10**, 1672–1684.

RUSAK, Z., JUDD, K. P. & WANG, S. 1997 The effect of small pipe divergence on near-critical swirling flows. *Phys. Fluids* **9**, 2273–2285.

RUSAK, Z., WANG, S. & WHITING, C. H. 1998*a* The evolution of a perturbed vortex in a pipe to axisymmetric vortex breakdown. *J. Fluid Mech.* **366**, 211–237.

RUSAK, Z., WHITING C. H. & WANG, S. 1998*b* Axisymmetric breakdown of a Q-vortex in a pipe. *AIAA J.* **36**, 659–667.

THOMPSON, P. A. 1988 *Compressible Fluid Dynamics.* Advanced Engineering Series.

WANG, S. & RUSAK, Z. 1996*a* On the stability of an axisymmetric rotating flow. *Phys. Fluids* **8**, 1007–1016.

WANG, S. & RUSAK, Z. 1996*b* On the stability of non-columnar swirling flows. *Phys. Fluids* **8**, 1017–1023.

WANG, S. & RUSAK, Z. 1997*a* The dynamics of a swirling flow in a pipe and transition to axisymmetric vortex breakdown. *J. Fluid Mech.* **340**, 177–223.

WANG, S. & RUSAK, Z. 1997*b* The effect of slight viscosity on near critical swirling flows. *Phys. Fluids* **9**, 1914–1927.